

Supplement: Inter-comparing Observations of Atmospheric HCl and Inferring the Global Cl_y Distribution

D.J. Lary^{1,2}, Darryn Waugh³, Anne Douglass², Rich Stolarski², Paul Newman²,
Mark Schoeberl², Hamse Mussa⁴

1. Equivalent PV latitude - potential temperature coordinates

Because a major component of the variability of trace gases is due to atmospheric transport it makes sense to use a co-ordinate system that ‘follows’ the large scale flow pattern to perform our analyses [Schoeberl *et al.*, 2000]. In this study Equivalent PV latitude - potential temperature coordinates are used.

Under adiabatic conditions air parcels move along isentropic surfaces (surfaces of constant potential temperature, θ) Taylor [1960]; Danielsen [1961, 1968]; Danielsen *et al.* [1970]. So when considering tracer fields θ is a suitable vertical coordinate. McIntyre and Palmer [1983, 1984]; Hoskins *et al.* [1985]; Hoskins [1991] have shown the value of isentropic maps of Ertel’s potential vorticity (PV) for visualising large scale dynamical processes. PV plays a central role in large scale dynamics where it behaves as an approximate material tracer Hoskins *et al.* [1985].

As a result, PV can be used as the horizontal spatial coordinate instead of latitude and longitude McIntyre [1980a, b]; Leovy *et al.* [1985]; Butchart and Remsburg [1986]; Schoeberl *et al.* [1989]; Schoeberl and Lait [1992]; Norton [1994]; Lary *et al.* [1995]. PV is sufficiently monotonic in latitude on an isentropic surface to act as a useful replacement coordinate for both latitude and longitude, reducing the tracer field from three dimensions to two. These ideas have already led to interesting studies correlating PV and chemical tracers such as N_2O and O_3 Schoeberl *et al.* [1989]; Proffitt *et al.* [1989]; Lait *et al.* [1990]; Douglass *et al.* [1990]; Proffitt *et al.* [1993]; Atkinson [1993]. A key result of these studies is that PV and ozone mixing ratios are correlated on isentropic surfaces in the lower stratosphere, as was first pointed out by Danielsen Danielsen [1968].

Since the absolute values of PV depend strongly upon height and the meteorological condition, it is useful to normalise PV and use equivalent PV latitude (ϕ_e) as the horizontal coordinate instead of PV itself. ϕ_e is calculated by considering the area enclosed within a given PV contour on a given θ surface. The ϕ_e assigned to every point on this PV contour is the latitude of a latitude circle which encloses the

same area as that PV contour. Therefore, for every level in the atmosphere ϕ_e has the same range of values, -90° to 90° . This provides a vortex-tracking, and indeed a flow-tracking, stratospheric coordinate system. In this study we have used UKMO meteorological analyses.

2. Using PDFs for Intercomparisons

A key issue in this paper is inter-comparing the various observational datasets. In the traditional approach to inter-comparison, we require coincidence in space and time. This strong constraint dramatically reduces the statistical sample sizes we can deal with. In addition, the definition of ‘coincident observations is not clearly defined.

Since the number of ‘coincidences in conventional satellite intercomparison is typically small, it is useful to take a complementary view that considerably relaxes the coincidence requirements, such as PDFs of trace gases. The PDFs of two sets of consistent measurements of the same trace gas should be the same, if the statistical ensembles are chosen appropriately. The requirement of strict spatial and temporal co-location is relaxed in favor of ‘statistical collocation’, in which ensembles of measurements are chosen so that they sample about the same geographical region at about the same time under the same dynamical conditions.

The PDFs give a clear indication of biases: they show up as a shift of the PDFs. To be effective, the method requires a sufficiently large ensemble of measurements. In this paper, we choose to consider an entire month of data and to specify the spatial domain in terms of equivalent PV latitude - potential temperature coordinates. In the scatter diagrams shown in the Figure 1 of the paper and Figure 1 of this supplement we plot the median values of the PDF of one instrument against the median values of the PDF of another instrument. The use of equivalent PV latitude - potential temperature coordinates is particularly useful in improving the effective latitudinal coverage of sparse observations such as those made by solar occultation or in-situ platforms. In this paper, our analysis starts with the launch of UARS and continues up to the present.

It is worth noting that PDFs have been used in a variety of tracer studies. These range from considering dispersing tropospheric pollutant plumes in the planetary boundary layer [Mylne and Mason, 1991; Rotach *et al.*, 1996; Georgiadis *et al.*, 1998; Franzese *et al.*, 1999; Ferrero *et al.*, 2001; Yee and Biltoft, 2004], running water channels [Bara *et al.*, 1992] and clouds [Yee *et al.*, 1994], pollutant emission rates [Ridolfi *et al.*, 2003] to tracer transport and stratospheric O_3 , CH_4 , N_2O , CO , CO_2 , and PV [Pierrehumbert, 1994; Yang, 1995; Sparling and Schoeberl, 1995; Sparling *et al.*, 1997; Rood *et al.*, 2000; Sparling, 2000; Pierrehumbert, 2000; Andrews *et al.*, 2001; Sparling and Bacmeister, 2001; Hu and Pierrehumbert, 2001, 2002; Gao *et al.*, 2002; Johnson *et al.*, 2002; Strahan, 2002; Neu *et al.*, 2003; Hsu *et al.*, 2004] tracer age and transit time [Holzer and Hall, 2000; Andrews *et al.*,

¹Goddard Earth Sciences and Technology Centre, University of Maryland Baltimore County, Baltimore, Maryland, USA

²Atmospheric Chemistry and Dynamics Branch, NASA, Goddard Space Flight Centre, Greenbelt, Maryland, USA

³The Department of Earth & Planetary Sciences Maryland, Johns Hopkins University, Baltimore, USA

⁴Department of Chemistry, University of Cambridge, England

2001; Holzer et al., 2003] and estimation of representativeness uncertainty in chemical data assimilation [Lary, 2003]. Using PDFs for validation has been found useful by the Aura instrument teams, for example [Froidevaux et al., 2005].

Not only does a PDF characterize the tracer distribution, its shape tells us about mixing barriers, how complete the mixing is, and chemical processes such as ozone depletion [Sparling [2000]; Pierrehumbert [2000]; Strahan [2002]; Neu et al. [2003]]. For example, a narrow peak in the concentration PDF indicates that the air is well mixed and significant variability generating processes have not recently occurred (e.g. long range transport). A multi-modal distribution indicates air of different origins (e.g. polar and mid-latitude). In general, broad peaks indicate recent variability generating processes such as photochemistry or transport (horizontal or vertical). Chemical processes such as ozone depletion will lead to an asymmetric broadening of the PDF towards low ozone values. Good examples of these different cases are shown for POAM observations of ozone by Strahan et al. [Strahan [2002]].

3. Neural Network

Neural networks are algorithms that can ‘learn’ the behavior of a wide variety of systems. The first computational model for an artificial neuron was proposed by McCulloch and Pitts in 1943. Neural networks have been trained to perform complex functions in diverse fields of application including pattern recognition, identification, classification, failure anticipation by public utilities, ionospheric forecasting, credit checking, speech and vision control systems, environmental studies, and tracer-tracer correlations [Krasnopolsky et al., 1995; Gemmill and Krasnopolsky, 1999; Müller et al., 2003; Lary and Mussa, 2004]. It is timely to extend the applications to infer the Cl_y distribution.

The general artificial neuron model has five components. The first thing an artificial neuron does is to compute the weighted sum of its inputs. The weights are real-valued numbers that determine the contribution of each input. The goal of neural network training algorithms is to determine the ‘best’ possible set of weight values for the problem under consideration. Finding the optimal set is often a trade-off between computation time, minimizing the network error, and maintaining the network’s ability to generalize. Depending on the goals, the complexity of neuron models may vary from simple threshold functions to complex simulations with thousands of variables described by complicated nonlinear equations.

Computational neural networks are composed of simple elements operating in parallel. Typically a neural network accepts a set of inputs in the input layer and provides a set of outputs in the output layer. Usually there are one or more hidden layers. The hidden layers are additional to the input and output layers and are not connected externally. The hidden layers are used to improve the performance of the neural network. As in nature, the network function is determined largely by the connections between elements. We can train a neural network to perform a particular function by adjusting the values of the connections (weights) between elements. Commonly neural networks are trained so that a particular input leads to a specific target output. In this supervised learning process, a large number of input/target pairs comprise the training data set, which should sample the entire input and output data space. The network weights are adjusted based on a comparison of the output and the target, either after presentation of each single pattern (incremental training) or all patterns in the training set (batch training). This procedure is repeated until the network output matches the target to the desired accuracy.

After the training has been done, the network can generalize these results to unknown input data, effectively performing a nonlinear, weighted, multi-dimensional interpolation.

In this study we use a multilayer perceptron feed-forward network with 20 nodes in the hidden layer and a non-linear output layer using a Kalman filter training algorithm. There was good convergence within 10 training epochs. A neural network was used as the mapping is multivariate and non-linear in HCl, equivalent PV latitude and potential temperature. The Kalman filter training algorithm [Lary and Mussa, 2004] was used for its excellent convergence behavior.

References

- Andrews, A. E., K. A. Boering, S. C. Wofsy, B. C. Daube, D. B. Jones, S. Alex, M. Loewenstein, J. R. Podolske, and S. E. Strahan, Empirical age spectra for the midlatitude lower stratosphere from in situ observations of CO_2 : Quantitative evidence for a subtropical ‘barrier’ to horizontal transport, *J. Geophys. Res. (Atmos.)*, 106(D10), 10,257–10,274, 2001.
- Atkinson, R., An observational study of the austral spring stratosphere: Dynamics, ozone transport and the ‘ozone dilution effect’, Ph.D. thesis, Massachusetts Institute of Technology, 1993.
- Bara, B. M., D. J. Wilson, and B. W. Zelt, Concentration fluctuation profiles from a water channel simulation of a ground-level release, *Atmospheric Environment*, 26(6), 1053–1062, 1992.
- Butchart, N., and E. E. Remsburg, The area of the stratospheric polar vortex as a diagnostic for tracer transport on an isentropic surface, *J. Atmos. Sci.*, 43(13), 1319–1339, 1986.
- Danielsen, E., Trajectories - isobaric, isentropic and actual, *Journal of Meteorology*, 18(4), 479–486, 1961.
- Danielsen, E., Stratospheric-tropospheric exchange based on radioactivity ozone and potential vorticity, *J. Atmos. Sci.*, 25(3), 502–, 1968.
- Danielsen, E., R. Bleck, Shedlovs.J, A. Wartburg, Haagenso.P, and W. Pollock, Observed distribution of radioactivity, ozone, and potential vorticity associated with tropopause folding, *J. Geophys. Res.*, 75(12), 2353–, 1970.
- Douglass, A., R. Rood, R. Stolarski, M. Schoeberl, M. Proffitt, J. Margitan, M. Loewenstein, J. Podolske, and S. Strahan, Global 3-dimensional constituent fields derived from profile data, *Geophys. Res. Lett.*, 17(4 SS), 525–528, 1990.
- Ferrero, E., D. Anfossi, and G. Tinarelli, Simulations of atmospheric dispersion in an urban stable boundary layer, *Int. J. Chem. Environ. Pollution*, 16(1-6), 1–8, 2001.
- Franzese, P., A. K. Luhan, and M. S. Borgas, An efficient lagrangian stochastic model of vertical dispersion in the convective boundary layer, *Atmospheric Environment*, 33(15), 2337–2345, 1999.
- Froidevaux, L., et al., Early validation analyses of atmospheric profiles from EOS MLS on the Aura satellite, *IEEE Trans. Geosci. Remote Sens.*, This issue, 2005.
- Gao, R. S., et al., Role of noy as a diagnostic of small-scale mixing in a denitrified polar vortex, *J. Geophys. Res. (Atmos.)*, 107(D24), 2002.
- Gemmill, W. H., and V. M. Krasnopolsky, The use of ssm/i data in operational marine analysis, *Weather and Forecasting*, 14(5), 789–800, 1999.
- Georgiadis, T., F. Fortezza, L. Alberti, V. Strocchi, A. Marani, and G. Dal Bo, Probability density functions of photochemicals over a coastal area of northern italy, *Nuovo Cimento Della Societa Italiana Di Fisica C-Geophysics and Space Physics*, 21(1), 75–84, 1998.
- Holzer, M., and T. M. Hall, Transit-time and tracer-age distributions in geophysical flows, *J. Atmos. Sci.*, 57(21), 3539–3558, 2000.
- Holzer, M., I. G. McKendry, and D. A. Jaffe, Springtime trans-pacific atmospheric transport from east asia: A transit-time probability density function approach, *J. Geophys. Res. (Atmos.)*, 108(D22), 2003.
- Hoskins, B., Towards a PV-Theta view of the general-circulation, *Tellus, Ser. A.*, 43(4), 27–35, 1991.

- Hoskins, B., M. McIntyre, and A. Robertson, On the use and significance of isentropic potential vorticity maps, *Q. J. R. Meteorol. Soc.*, 111(470), 877–946, 1985.
- Hsu, J., M. J. Prather, O. Wild, J. K. Sundet, I. S. A. Isaksen, E. V. Browell, M. A. Avery, and G. W. Sachse, Are the trace-p measurements representative of the western pacific during march 2001?, *J. Geophys. Res. (Atmos.)*, 109(D2), 2004.
- Hu, Y., and R. T. Pierrehumbert, The advection-diffusion problem for stratospheric flow. part i: Concentration probability distribution function, *J. Atmos. Sci.*, 58(12), 1493–1510, 2001.
- Hu, Y. Y., and R. T. Pierrehumbert, The advection-diffusion problem for stratospheric flow. Part II: Probability distribution function of tracer gradients, *J. Atmos. Sci.*, 59(19), 2830–2845, 2002.
- Johnson, D. R., A. J. Lenzen, T. H. Zapotocny, and T. K. Schaack, Numerical uncertainties in simulation of reversible isentropic processes and entropy conservation: Part II, *J. Clim.*, 15(14), 1777–1804, 2002.
- Krasnopolsky, V. M., L. C. Breaker, and W. H. Gemmill, A neural-network as a nonlinear transfer-function model for retrieving surface wind speeds from the special sensor microwave imager, *Journal of Geophysical Research-Oceans*, 100(C6), 11,033–11,045, 1995.
- Lait, L., et al., Reconstruction of O₃ and N₂O fields from ER-2, DC-8, and balloon observations, *Geophys. Res. Lett.*, 17(4 SS), 521–524, 1990.
- Lary, D., Representativeness uncertainty in chemical data assimilation highlight mixing barriers, *Atmos. Sci. Lett.*, 5(1-4), 35–41, 2003.
- Lary, D., M. Chipperfield, J. Pyle, W. Norton, and L. Riishojgaard, 3-dimensional tracer initialization and general diagnostics using equivalent PV latitude-potential-temperature coordinates, *Q. J. R. Meteorol. Soc.*, 121(521 PtA), 187–210, 1995.
- Lary, D. J., and H. Y. Mussa, Using an extended kalman filter learning algorithm for feed-forward neural networks to describe tracer correlations, *Atmospheric Chemistry and Physics Discussions*, 4, 3653–3667, 2004.
- Leovy, C. B., C. R. Sun, M. H. Hitchman, E. E. Remsberg, J. M. Russell, L. L. Gordley, J. C. Gille, and L. V. Lyjak, Transport of ozone in the middle stratosphere - evidence for planetary wave breaking, *J. Atmos. Sci.*, 42(3), 230–244, 1985.
- McIntyre, M., and T. Palmer, Breaking planetary-waves in the stratosphere, *Nature*, 305(5935), 593–600, 1983.
- McIntyre, M., and T. Palmer, The surf zone in the stratosphere, *J. Atmos. Terr. Phys.*, 46(9), 825–849, 1984.
- McIntyre, M. E., Towards a lagrangian-mean description of stratospheric circulations and chemical transports, *Phil. Tran. R. Soc. London Series A-Math. Phys. Eng. Sci.*, 296(1418), 129–148, 1980a.
- McIntyre, M. E., An introduction to the generalized lagrangian-mean description of wave, mean-flow interaction, *Pure Appl. Geophys.*, 118(1-2), 152–176, 1980b.
- Müller, M. D., A. K. Kaifel, M. Weber, S. Tellmann, J. P. Burrows, and D. Loyola, Ozone profile retrieval from global ozone monitoring experiment (gome) data using a neural network approach (neural network ozone retrieval system (nnorsy)), *J. Geophys. Res. (Atmos.)*, 108(D16), 2003.
- Mylne, K. R., and P. J. Mason, Concentration fluctuation measurements in a dispersing plume at a range of up to 1000-m, *Q. J. R. Meteorol. Soc.*, 117(497), 177–206, 1991.
- Neu, J. L., L. C. Sparling, and R. A. Plumb, Variability of the subtropical "edges" in the stratosphere, *J. Geophys. Res. (Atmos.)*, 108(D15), 2003.
- Norton, W., Breaking rossby waves in a model stratosphere diagnosed by a vortex-following technique for advecting material contours, *J. Atmos. Sci.*, 51(4), 654–673, 1994.
- Pierrehumbert, R. T., Tracer microstructure in the large-eddy dominated regime, *Chaos Solitons & Fractals*, 4(6), 1091–1110, 1994.
- Pierrehumbert, R. T., Lattice models of advection-diffusion, *Chaos*, 10(1), 61–74, 2000.
- Proffitt, M., K. Aikin, J. Margitan, M. Loewenstein, J. Podolske, A. Weaver, K. Chan, H. Fast, and J. Elkins, Ozone loss inside the northern polar vortex during the 1991-1992 winter, *Science*, 261(5125), 1150–1154, 1993.
- Proffitt, M., et al., Insitu ozone measurements within the 1987 antarctic ozone hole from a high-altitude ER-2 aircraft, *J. Geophys. Res. (Atmos.)*, 94(D14), 16,547–16,555, 1989.
- Ridolfi, L., P. D'Odorico, A. Porporato, and I. Rodriguez-Iturbe, The influence of stochastic soil moisture dynamics on gaseous emissions of NO, N₂O, and N₂, *Hydro. Sci. J.*, 48(5), 781–798, 2003.
- Rood, R. B., A. R. Douglass, M. C. Cerniglia, L. C. Sparling, and J. E. Nielsen, Seasonal variability of middle-latitude ozone in the lowermost stratosphere derived from probability distribution functions, *J. Geophys. Res. (Atmos.)*, 105(D14), 17,793–17,805, 2000.
- Rotach, M. W., S. E. Gryning, and C. Tassone, A two-dimensional lagrangian stochastic dispersion model for daytime conditions, *Q. J. R. Meteorol. Soc.*, 122(530), 367–389, 1996.
- Schoeberl, M., and L. Lait, Conservative-coordinate transformations for atmospheric measurements, in *Use of EOS for Studies of Atmospheric Physics*, vol. 115th course of the international school of physics Enrico Fermi, pp. 419–431, 1992.
- Schoeberl, M. R., L. C. Sparling, C. H. Jackman, and E. L. Fleming, A lagrangian view of stratospheric trace gas distributions, *J. Geophys. Res. (Atmos.)*, 105(D1), 1537–1552, 2000.
- Schoeberl, M. R., et al., Reconstruction of the constituent distribution and trends in the antarctic polar vortex from er-2 flight observations, *J. Geophys. Res. (Atmos.)*, 94(D14), 16,815–16,845, 1989.
- Sparling, L. C., Statistical perspectives on stratospheric transport, *Rev. Geophys.*, 38(3), 417–436, 2000.
- Sparling, L. C., and J. T. Bacmeister, Scale dependence of tracer microstructure: Pdfs, intermittency and the dissipation scale, *Geophys. Res. Lett.*, 28(14), 2823–2826, 2001.
- Sparling, L. C., and M. R. Schoeberl, Mixing entropy analysis of dispersal of aircraft emissions in the lower stratosphere, *J. Geophys. Res. (Atmos.)*, 100(D8), 16,805–16,812, 1995.
- Sparling, L. C., J. A. Kettleborough, P. H. Haynes, M. E. McIntyre, J. E. Rosenfield, M. R. Schoeberl, and P. A. Newman, Diabatic cross-isentropic dispersion in the lower stratosphere, *J. Geophys. Res. (Atmos.)*, 102(D22), 25,817–25,829, 1997.
- Strahan, S., Influence of planetary wave transport on arctic ozone as observed by polar ozone and aerosol measurement (poam) iii, *J. Geophys. Res. (Atmos.)*, 107(D20), 2002.
- Taylor, R., The topography of the 400k isentropic surface over antarctica: Spring 1957, IGY Report Number 11, National Academy Sciences, 1960.
- Yang, H. J., 3-dimensional transport of the ertel potential vorticity and N₂O in the GFDL skyhi model, *J. Atmos. Sci.*, 52(9), 1513–1528, 1995.
- Yee, E., and C. A. Biltoft, Concentration fluctuation measurements in a plume dispersing through a regular array of obstacles, *Boundary-Layer Met.*, 111(3), 363–415, 2004.
- Yee, E., R. Chan, P. R. Kosteniuk, G. M. Chandler, C. A. Biltoft, and J. F. Bowers, Concentration fluctuation measurements in clouds released from a quasi-instantaneous point-source in the atmospheric surface-layer, *Boundary-Layer Met.*, 71(4), 341–373, 1994.

D.J. Lary, Goddard Earth Sciences and Technology Centre, University of Maryland Baltimore County, Baltimore, MD 21228 (David.Lary@umbc.edu)

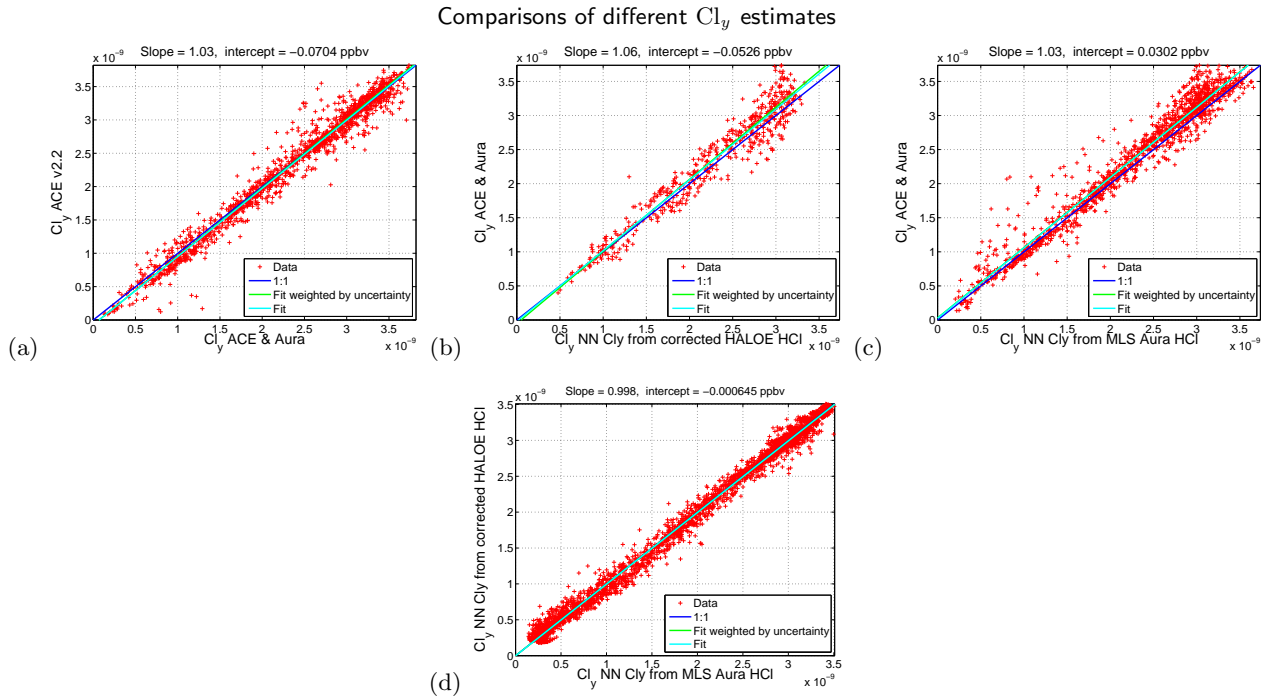


Figure 1. Panel (a) shows a scatter plot of all contemporaneous Cl_y observations made by ACE v2.2 (i.e. $HCl+ClONO_2$) compared to the Cl_y estimate when we use Aura MLS HCl instead of ACE v2.2 HCl. As would be expected from the paper’s Figure 1 panel (g) there is good agreement between the two Cl_y estimates. Good agreement within the measurement uncertainties. If we now use the observed HCl from UARS HALOE or Aura MLS and the neural network to infer Cl_y we also get good agreement with the observed Cl_y as can be seen in panels (b) and (c). Finally, if we compare the two neural network estimates based on UARS HALOE HCl and Aura MLS HCl we also get good agreement as can be seen in panel (d). The dark blue line in each case is the ideal 1:1 curve if the instruments were agreeing perfectly. The green and cyan lines are linear fits with and without accounting for the observation uncertainties.

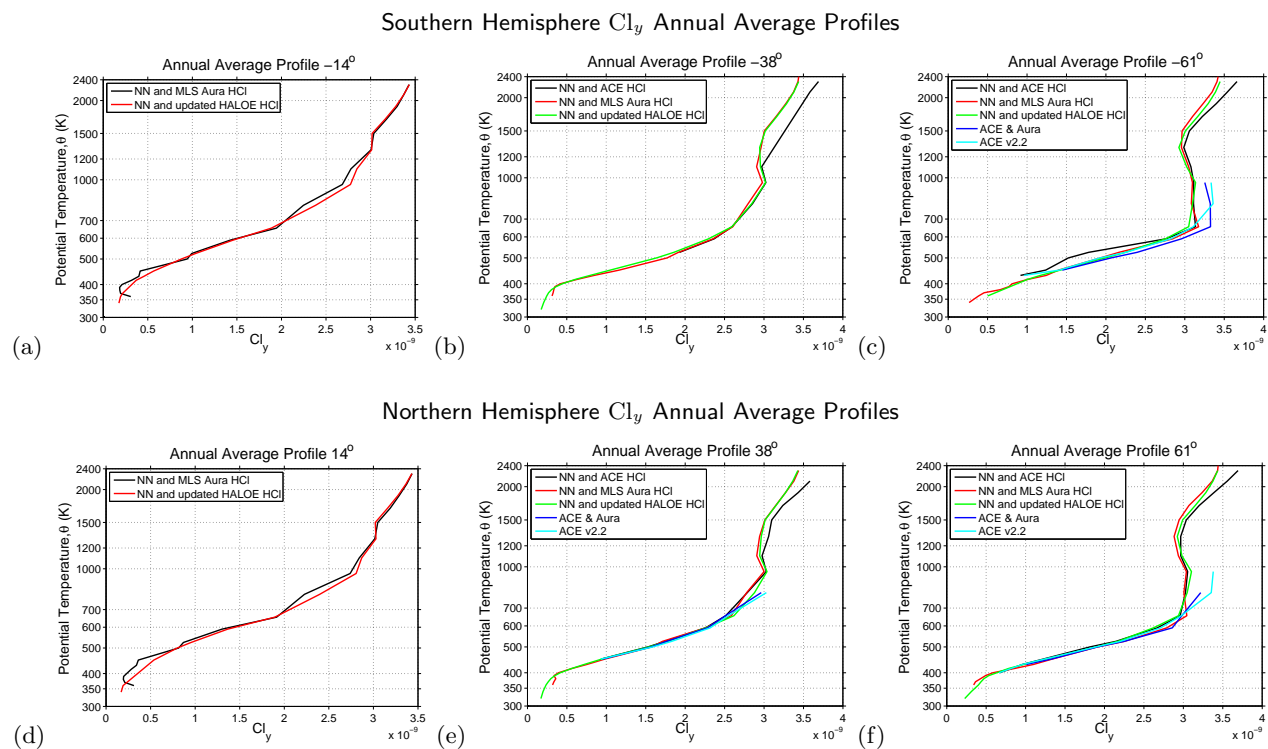


Figure 2. Panels (a) and (c) show annual average profiles of different Cl_y estimates for the southern hemisphere. Panels (d) and (e) show the corresponding profiles for the northern hemisphere. The effects of the limited training data set for the neural network mapping from HCl to Cl_y is evident at higher latitudes above the 700 K isentropic surface. This will no doubt be improved as the length of the data record from ACE increases.